The Formation Mechanism Of Compacted/Vermicular Graphite in Cast Irons

H. Itofuji
Kyoto University, Kyoto, Japan (Ube Industries, Ltd.)
Y. Kawano
N. Inoyama
S. Yamamoto
Kyoto University, Kyoto, Japan
B. Chang
QIT-Fer et Titane, Inc., Tokyo, Japan
T. Nishi
Ube Industries, Ltd., Ube City, Japan

ABSTRACT

To clarify the mechanism of compacted/vermicular (C/V) graphite formation in cast irons, the solidification process was studied. Small specimens of C/V graphite cast irons were quenched at selected temperatures during the solidification and then the metallographic observations were carried out. The same experiment was done for spheroidal graphite cast iron in order to compare with the formation process of C/V graphite. The main results are summarized.

1) *No difference was observed at the early stage of solidification between C/V graphite formation and spheroidal graphite formation, i.e., only tiny graphite nodules were formed in the melt.*
2) *After being surrounded by austenite shell, C/V graphite grew preferentially along austenite grain boundaries, which act as carbon feed channels from the surrounding liquid in contact with the liquid, while spheroidal graphite continued to grow uniformly in a radial direction by lattice diffusion of iron atoms because of isolation from the liquid.*
3) *Repeated polishing and examination revealed that C/V graphite was interconnected throughout the austenite shell and that the branches of C/V graphite were connected to the original graphite nodule in most of the metallographic observations.*

INTRODUCTION

Since C/V graphite cast irons are obtained by magnesium (Mg) or Cerium (Ce) treatment in the same way as spheroidal graphite cast irons, the mechanism of C/V graphite formation is expected to be similar to that of spheroidal graphite. Of late, there have been many papers[1-40] on C/V graphite cast irons, whereas the mechanism of its formation has not been well understood. Htum[2] and Liu, et al,[19,22] have discussed the growth behavior of C/V graphite to some extent, but their explanations are not enough to elucidate the mechanism of C/V graphite formation.

In the present work, some experiments were carried out to clarify the mechanism based upon the gas bubble theory[41-50] of spheroidization of graphite in cast irons. According to the gas bubble theory, graphite nodules are formed as a result of the precipitation of graphite into the gas bubble such as Mg and hydrogen and they continue to grow centrifugally after filling up gas bubbles with graphite. If the centrifugal growth proceeds uniformly, graphite nodules still remain spheroidal. Otherwise, the shape of the graphite nodules will be degenerated. Accordingly, in this paper, discussion on C/V graphite formation is focused on degeneration of graphite nodule during the process of outward growth.

Judging from these experimental results, it is clear that C/V graphite formation results from the degeneration of graphite nodule in the process of outward growth.

EXPERIMENTAL PROCEDURE

Synthetic cast irons, prepared from electrolytic iron containing 0.005% C, 0.005% Mn, 0.004% P, 0.005% S and 0.004% Cu as impurities, carbon of 99.998% and metallic silicon of 99.999% were used as base metals in the present work. They were melted with a Kryptol Furnace. The melts were poured into permanent molds 10 mm (0.394 in.) in diameter and 100 mm (3.940 in.) in length. The chemical compositions are given in Table 1. The remelting and treatment apparatuses are presented in Figs. 1 and 2, respectively.

Table 1. Chemical Composition of Base Metals

Base Metal	C	Si	Mn	P	S
CV-1	3.22	2.79	0.01	0.002	0.007
CV-2	3.43	1.95	0.01	0.002	0.011
CV-3	3.56	2.46	0.01	0.002	0.025

The base metals were remelted (air melt) in high purity graphite crucibles using an electric resistance furnace. Two types of C/V graphite cast irons were produced to investigate

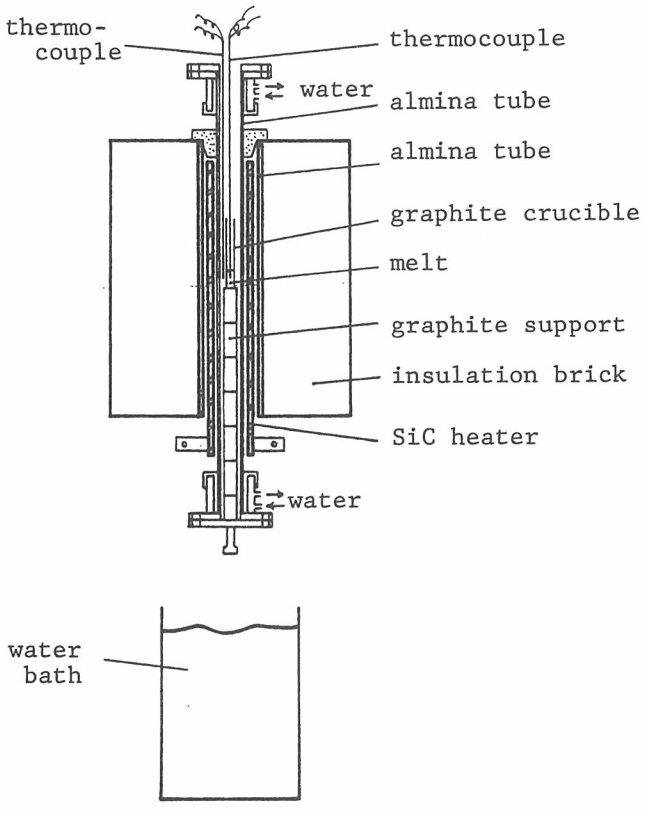

Fig. 1. Experimental apparatus for remelting and quenching.

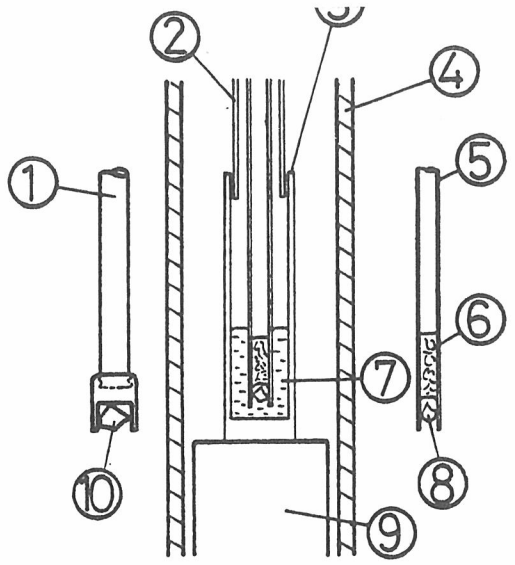

1.graphite phosphorizer
2.silica tube
3.graphite crucibe (ϕ12×15,ϕ18×23)
4.almina tube
5.silica phosphorizer
6.glass wool
7.melt
8.50%Ce-mish metal
9.graphite support
10.Fe-Si-5.5%Mg

Fig. 2. Experimental apparatus for vermiculization and spheroidization.

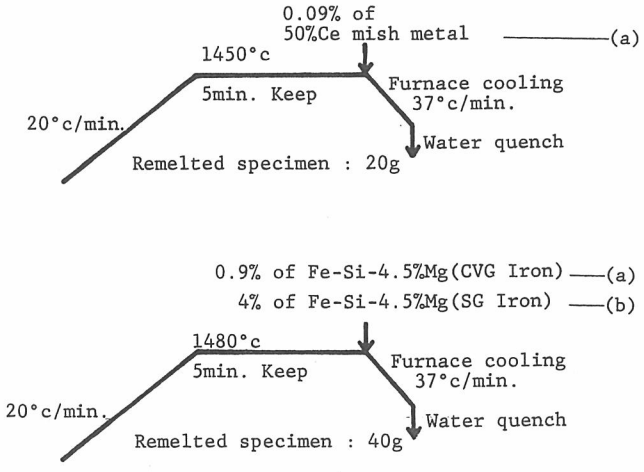

Fig. 3. Conditions of remelting, treatment and quenching for C/V graphite cast iron (a); and spheroidal graphite cast iron (b).

was treated with 50% Ce mish metal and another with Fe-Si-4.5% Mg. The conditions of remelting, treatment and quenching are shown in Fig. 3. The Fe-Si-Mg alloy was preheated for about 2 min at 1000C (1832F), in the same furnace, to minimize the temperature drop of the melts by its addition. For Ce mish metal, no preheating was needed before the treatment because of its small addition. After vermiculization, the melts were soon cooled at the rate of around 37C/min and subsequently quenched into a water bath at selected temperatures during the solidification. These quenched samples were subjected to optical metallographic examination.

Two Pt-13% PtRh thermocouples were used for the temperature control; one for the furnace and another for the

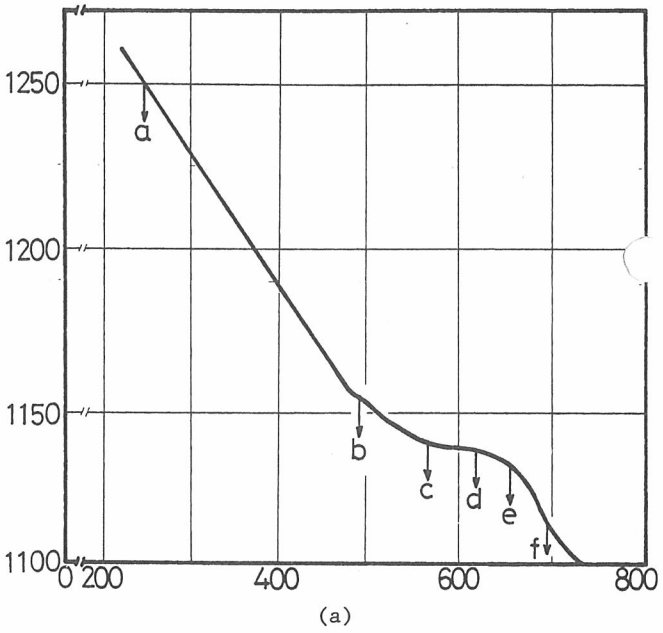

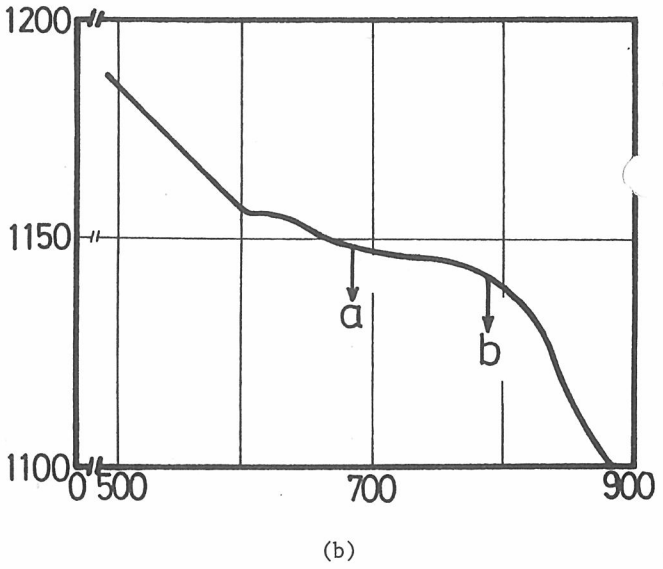

Fig. 4. Cooling curves and quenching times for alloy CV-1 and alloy CV-3: a) alloy CV-1 was remelted and then treated with 0.09% of 50% Ce mish metal; b) alloy CV-3 was remelted and then treated with 0.9% of Fe-Si-4.5% Mg.

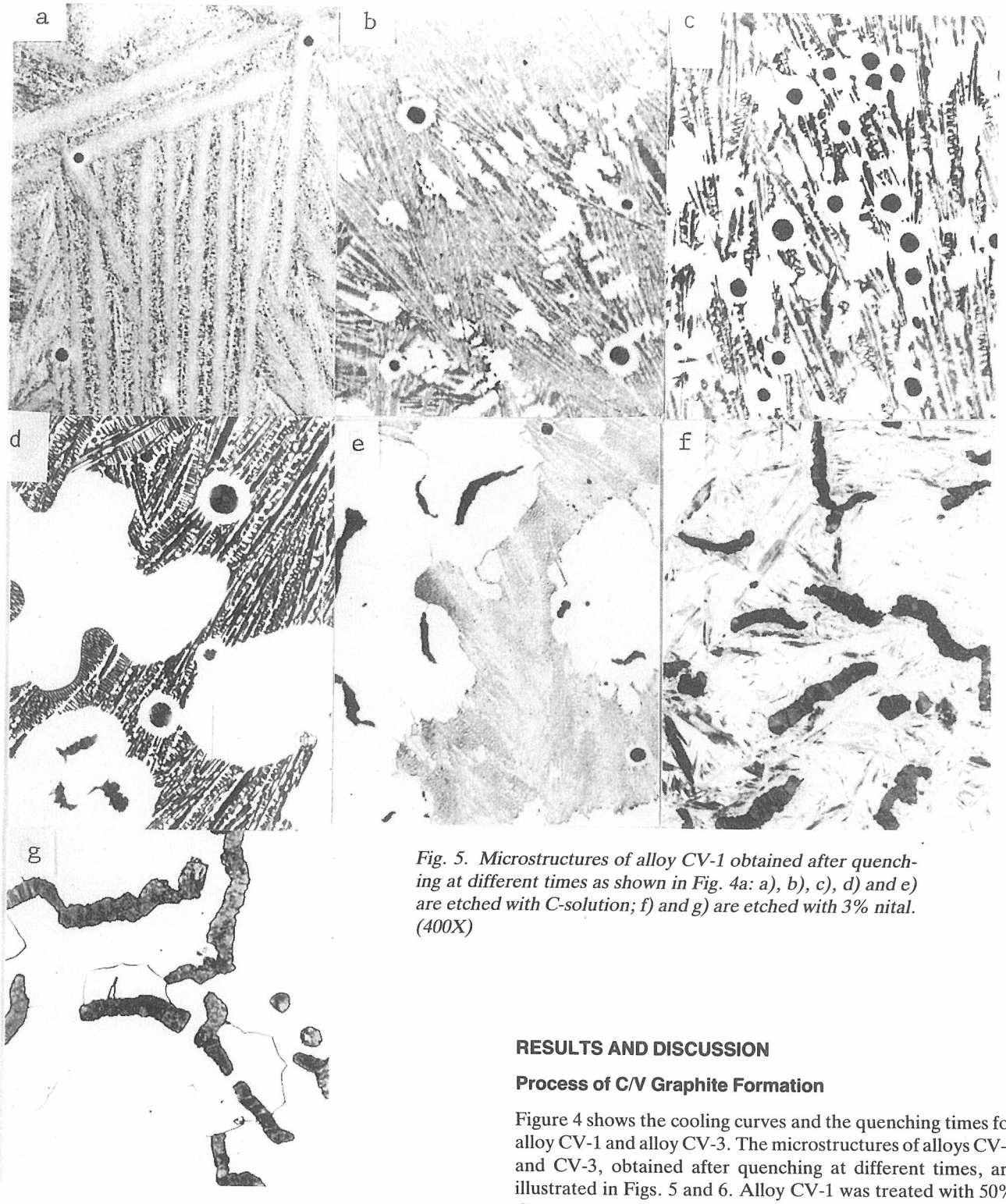

Fig. 5. Microstructures of alloy CV-1 obtained after quenching at different times as shown in Fig. 4a: a), b), c), d) and e) are etched with C-solution; f) and g) are etched with 3% nital. (400X)

specimens. The latter was positioned in the center of the melt after the treatment and the cooling curve was recorded.

Metallographic specimens of spheroidal graphite cast iron was also prepared in the same way as C/V graphite cast iron, as presented in Fig. 3b.

For metallographic observation, all quenched specimens were etched with C - solution[50] containing: 10g sodium hydroxide; 0.2g picric acid; and 100cc water, i.e., only the cementite was etched. Non-quenched samples were etched with 3% nital.

RESULTS AND DISCUSSION

Process of C/V Graphite Formation

Figure 4 shows the cooling curves and the quenching times for alloy CV-1 and alloy CV-3. The microstructures of alloys CV-1 and CV-3, obtained after quenching at different times, are illustrated in Figs. 5 and 6. Alloy CV-1 was treated with 50% Ce mish metal and alloy CV-3 was treated with Fe-Si-4.5% Mg. It was observed that there was no significant difference on the process of C/V graphite formation between 50% Ce mish metal and Fe-Si-4.5% Mg treatment. Since both microstructures observed were similar, the further explanation was limited on the results of alloy CV-1. On quenching at the a-point of Fig. 4(1), the melt was dropped onto an inclined metal plate which was set in a water bath to make it possible to quench it effectively.

The droplet specimen obtained in this way was about 2 mm (0.079 in.) in diameter and only graphite nodules without

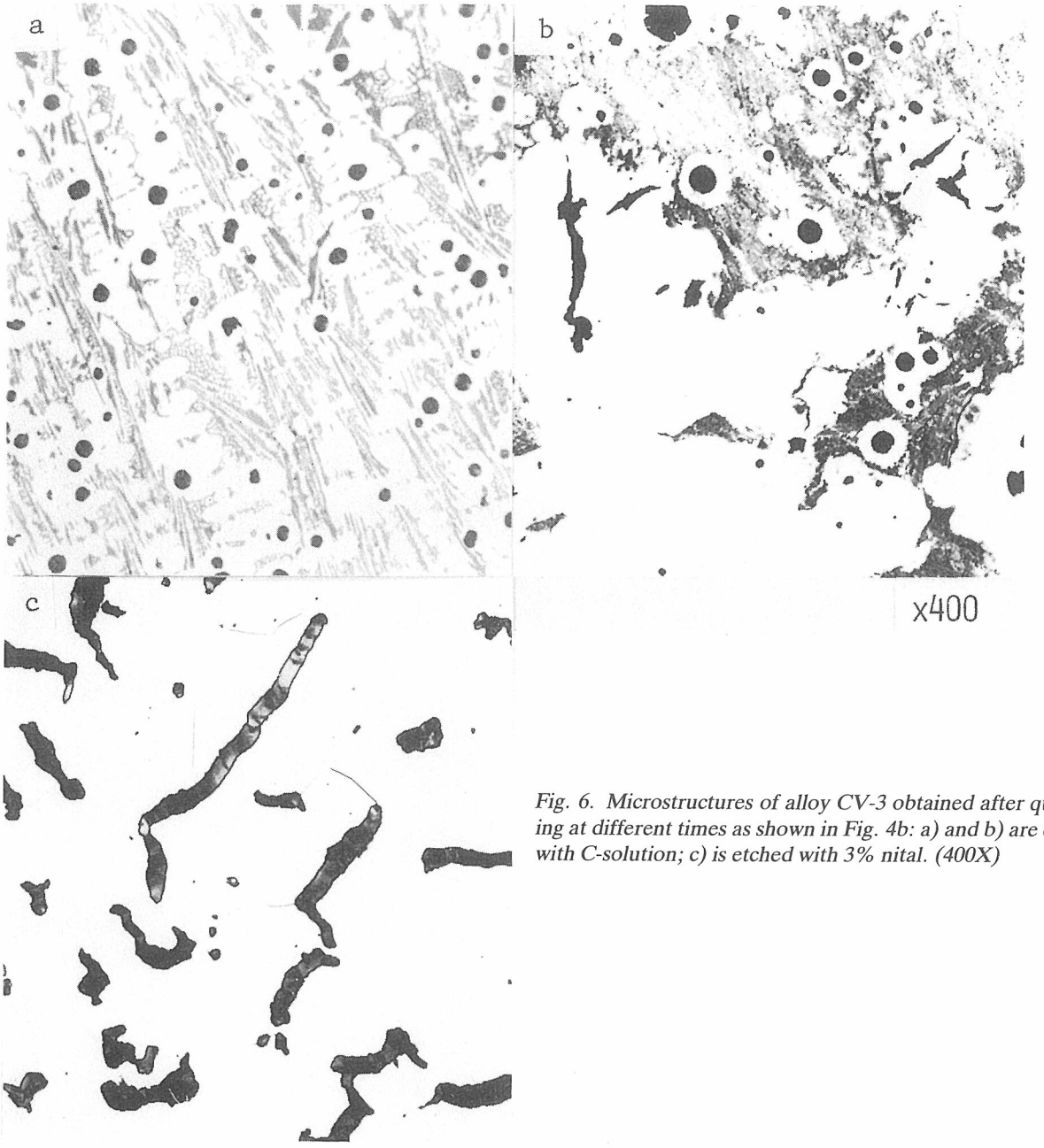

Fig. 6. Microstructures of alloy CV-3 obtained after quenching at different times as shown in Fig. 4b: a) and b) are etched with C-solution; c) is etched with 3% nital. (400X)

austenite shells were observed within it, as presented in Fig. 5a. It is very likely that these graphite nodules were precipitated before the eutectic solidification. Micrographs at a later stage, Fig. 5b, show that most of the nodules are enveloped by austenite shells. These findings indicate that only graphite nodules originate in the melt at the pre-eutectic temperature and the early stage of the eutectic solidification in C/V graphite cast iron, as in the case of spheroidal graphite cast iron.

With the progress of the solidification, graphite nodules started to grow into C/V graphite in austenite shell and continued until the completion of the eutectic solidification, as shown in Figs. 5d and 5e. It is worth noticing that graphite nodules were also observed within the residual melt, even in the specimens quenched at the late solidification process.

The total number of graphite nodules, however, was reduced as compared with the early stage of the solidification.

Fig. 5f presents the microstructure of the specimen quenc just after the eutectic soldification, where the graphite structure is the same as the as-cast one (Fig. 5g). The graphite morphology within a eutectic austenite shell was investigated by repeated polishing and examination on 20 views to understand the relationships between the original graphite nodule and C/V graphite growth.

Alloy CV-2 was treated with 50% Ce mish metal and followed by the addition of 8% Mn and 4% Ni. Then, the melt was quenched during the eutectic solidification. The addition of austenizers, Ni and Mn, was to avoid transformation of austenite during quenching and this treatment was needed to observe grain boundaries in austenite shell. Micrographs in Fig. 7 present selected graphite morphologies during C/V graphite growth process. In this micrographic study, C/V graphite phases were apparently interconnected with each other within a shell and the branches of C/V graphite were connected to the graphite nodule.

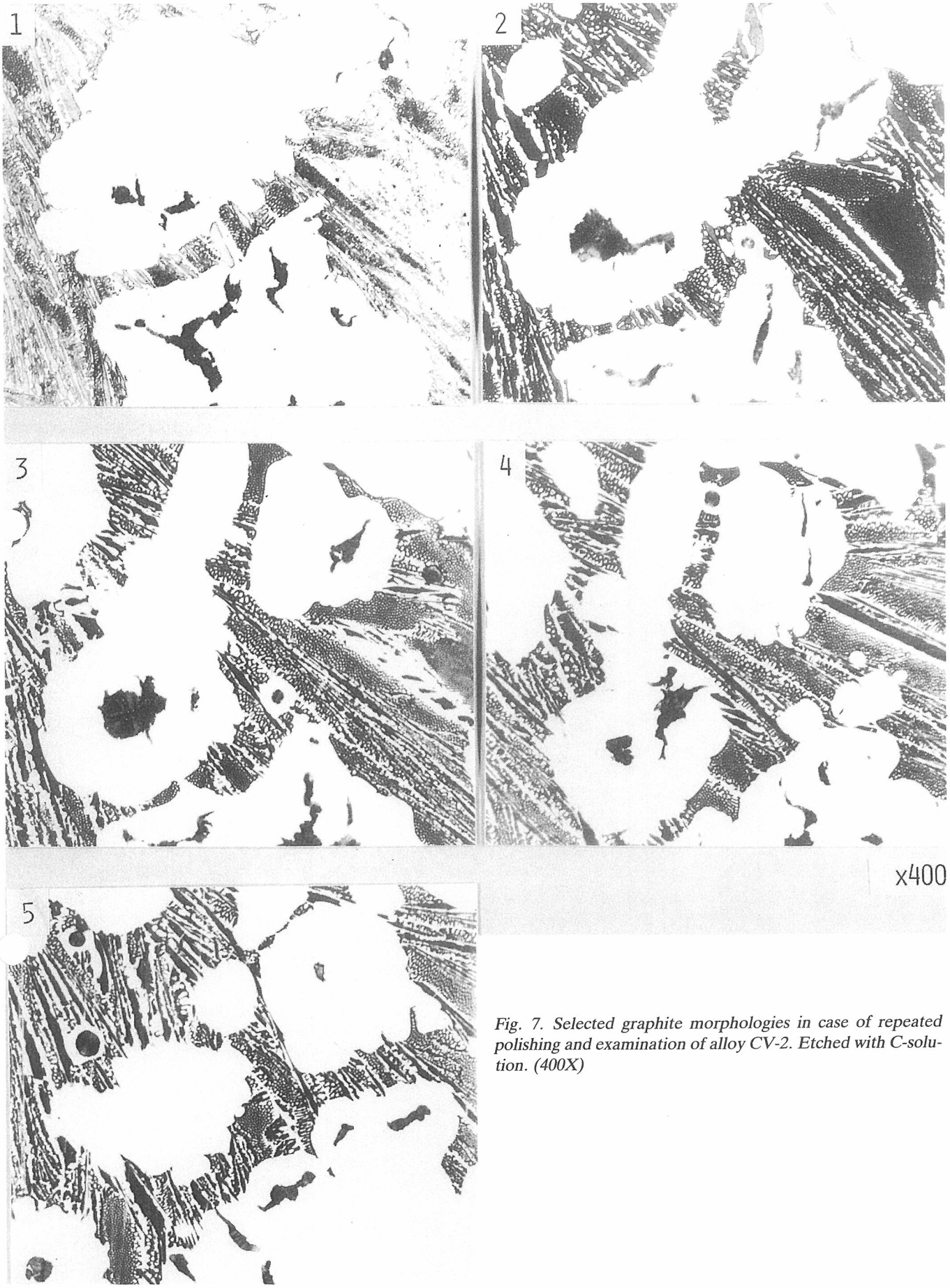

Fig. 7. Selected graphite morphologies in case of repeated polishing and examination of alloy CV-2. Etched with C-solution. (400X)

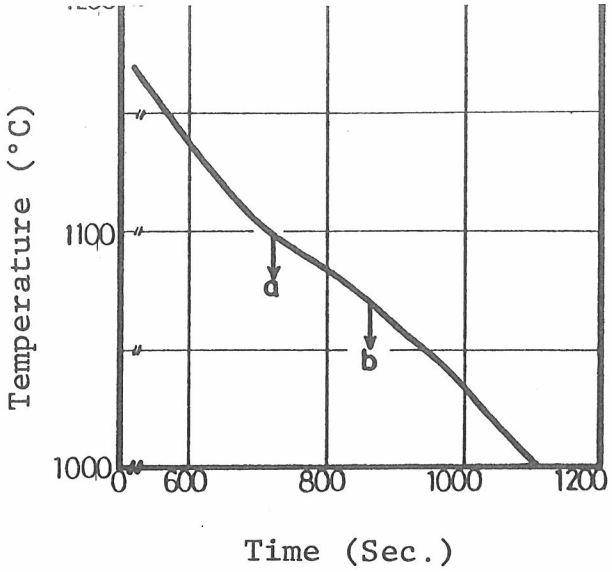

Fig. 8. Cooling curve and quenching times for spheroidal graphite cast iron treated with 4% of Fe-Si-4.5% Mg.

phenomenon. Consequently, it is concluded that graphite nodule precipitates as the primary form of C/V graphite, followed by growth of flaky graphites from it.

Process of Spheroidal Graphite Formation

The cooling curve and the quenching times for spheroidal graphite cast iron are presented in Fig. 8. Figure 9 shows the microstructures of the quenched specimens. In the specimen quenched at the a-point, graphite nodules with a size below 10 μ m and enveloped by austenite shells, were observed as presented in Fig. 9a.

Since graphite nodule precipitates as the primary form, even in C/V graphite cast iron, it is natural that graphite nodules should appear in spheroidal graphite cast iron melt. Some investigators[2,5,51,52] have pointed out that graphite nodule originates in the melt; however, they never explain why it does. This fact will be discussed later. It was observed that spheroidal graphite grew in austenite shell, as shown in Fig. 9b. Figure 9c shows the as-cast structure.

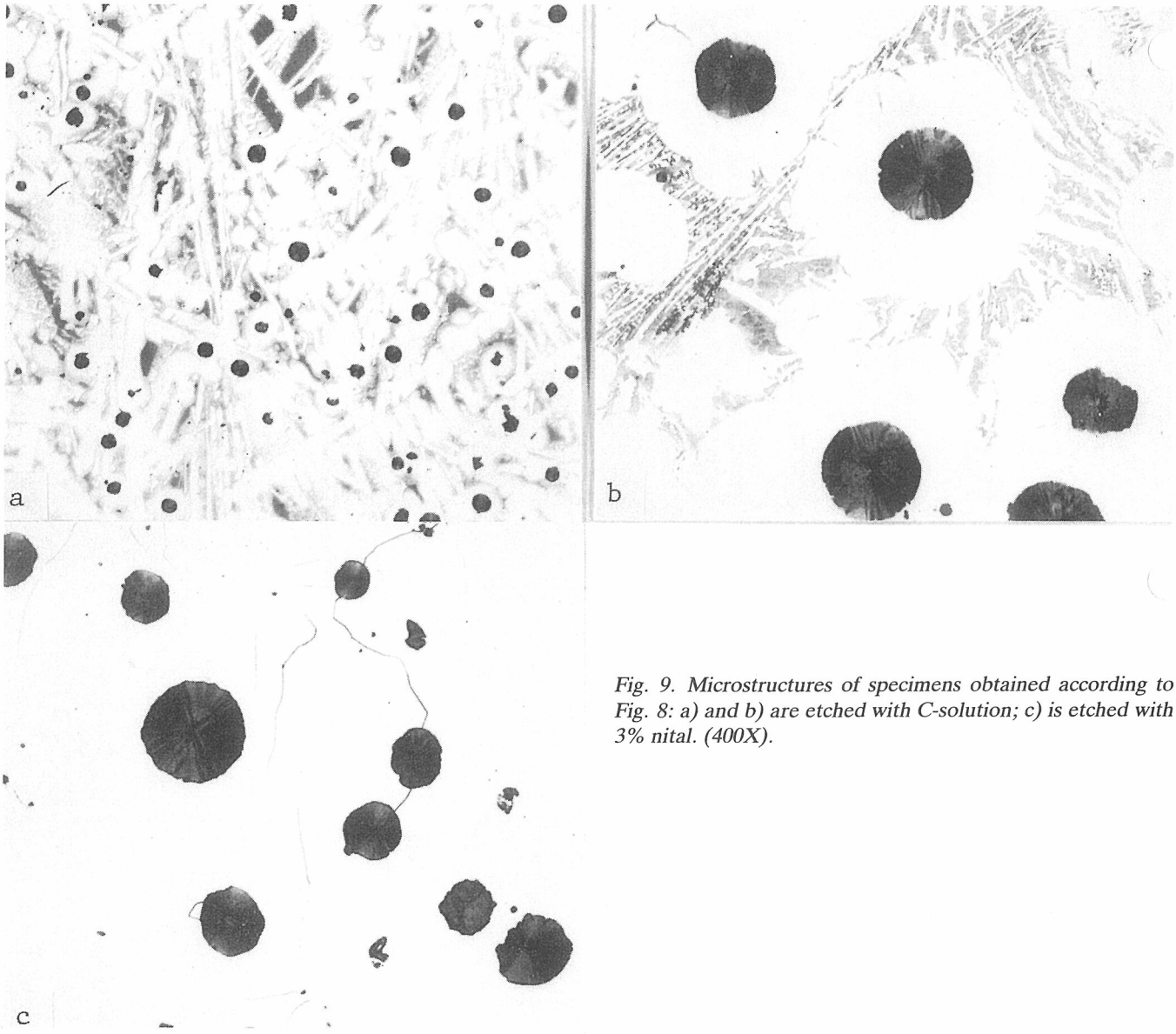

Fig. 9. Microstructures of specimens obtained according to Fig. 8: a) and b) are etched with C-solution; c) is etched with 3% nital. (400X).

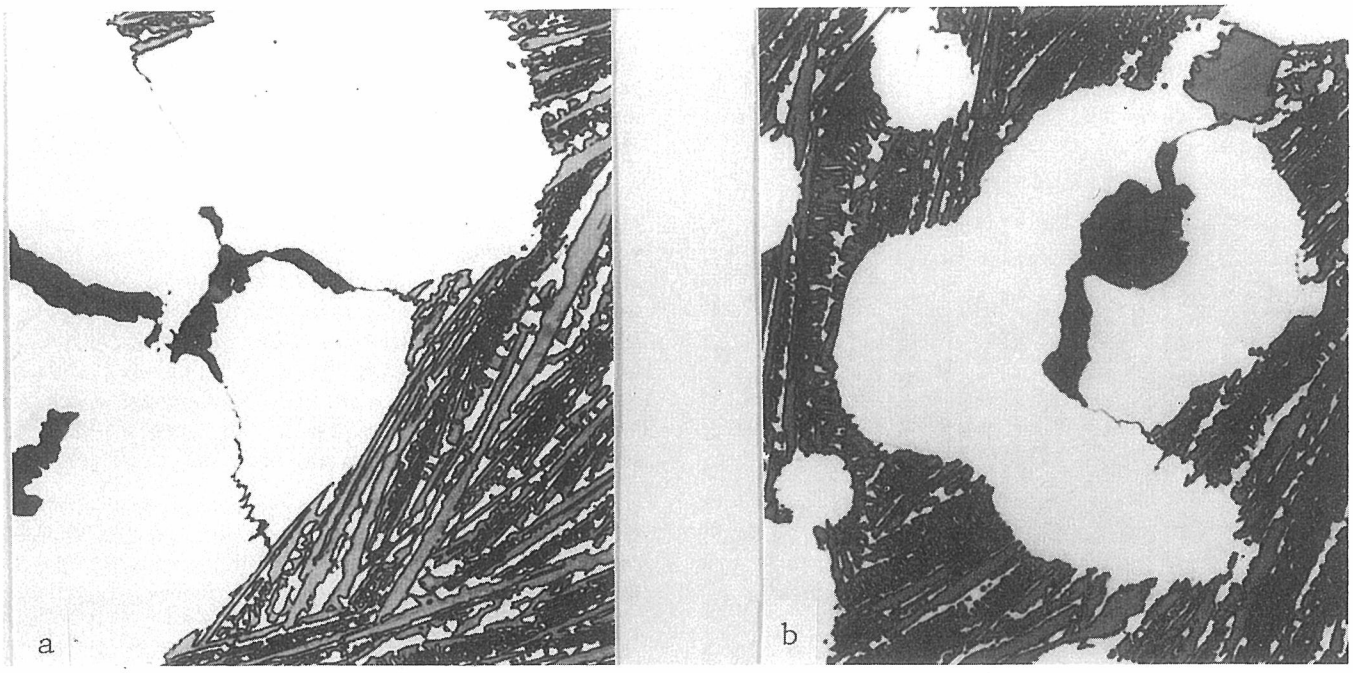

Fig. 10. After the addition of 8% Mn and 4% Ni, CV-2 was treated with 0.09% of 50% Ce mish metal. Etched with C-solution. (800X)

Difference Between C/V and Spheroidal Graphite Growth

It was obvious that the primary form of C/V and spheroidal graphite was quite the same at the initial stage. However, their final shapes came to differ from each other with the proceeding of solidification.

The relationships between graphite morphology and austenite structure, during the eutectic solidification of the two types of cast irons, were investigated in more detail in order to clarify the reason why original graphite nodule grows into different shapes. These results were presented in Figs. 10 and 11, respectively.

As shown in Fig. 10, it was observed that the tips of C/V graphite, during the growth, were connected to the melt through thin liquid channels and that C/V graphite grew preferentially along these channels. Figure 10b shows that graphite nodule is connected to C/V graphite.

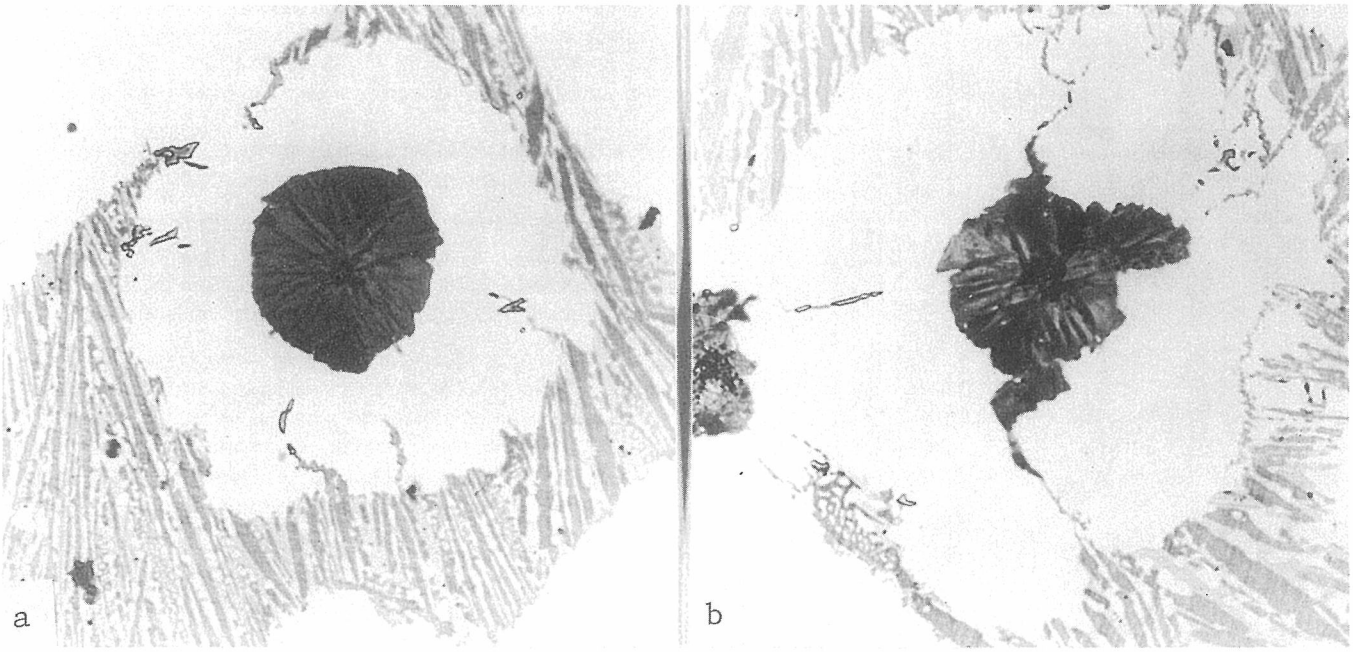

Fig. 11. Observation of the eutectic austenite shell with spheroidal graphite. After the addition of 8% Mn and 4% Ni, CV-3 was treated with 4% of Fe-Si-4.5% Mg. Etched with C-solution. (800X)

spheroidal graphite was completely isolated from the melt and that degenerated spheroidal graphite was also connected to the melt, as in the case of C/V graphite, as shown in Fig. 11b. Htun[2] and Aleksandrov[5] have also reported about this phenomenon.

Formation of Thin Liquid Channel

As Horie[53] pointed out, a thin liquid channel may be formed due to the segregation of impurities, such as Ti, Al, B, Cu, Sn,

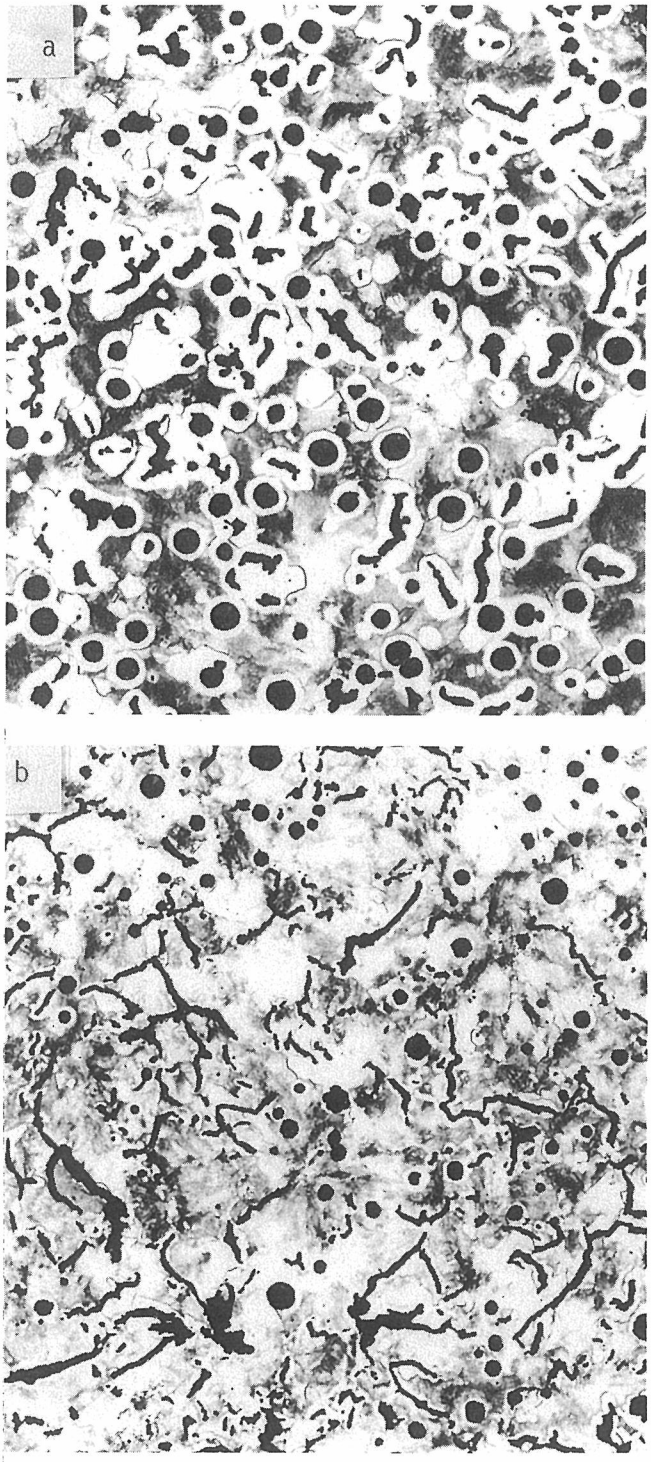

Fig. 12. Influence of Sn as impurity. Cast iron with 3.56% C, 2.46% Si, 0.01% Mn, 0.002% P, 0.012% S: a) 0.012% Ce; b) 0.015% Ce, 0.10% Sn. Etched with 3% nital. (100X)

austenite shell forms around graphite nodule, the impurities are rejected from austenite phase. Consequently, austenite grain or cell boundary is so enriched in the impurities, that the melting point drops,[54] resulting in formation of a thin liquid channel. O and S may also be related to form the channel.

The influence of Sn is presented in Fig. 12 as one example. Figure 12a shows the microstructure of the specimen, which was cast into a CO_2 mold 30 mm (1.181 in.) in diameter, just after spheroidization and inoculation without Sn-addition, while Fig. 12b shows the microstructure of the specimen, cast into the same mold as the above, after the addition of 0.1% Sn. It was observed that, as a result of the addition of 0.1% Sn, the number of C/V graphite increased and the length was much longer than usual. This observation suggests that Sn segregated and condensed at austenite grain or cell boundary.

In addition, it is well known in practical production of C/V graphite cast iron that C/V graphite structure can be obtained effectively and somewhat consistently by the addition of Fe-Si-Mg alloy containing Ti. Moreover, it is also well known that rapid cooling of C/V graphite cast iron melt leads to the production of spheroidal graphite cast iron. This may be because rapid cooling does not allow impurities to segregate, resulting in the formation of spheroidal graphite.

GENERAL DISCUSSION

C/V and Spheroidal Graphite Formation

As the results of this study, the formation process of C/V and spheroidal graphite is schematically illustrated in Fig. 13. The process is explained as follows. Precipitation of graphite occurs at surface of gas bubble, which is introduced by spheroidizers such as Mg and Ce alloys, because of the free site; thus, the graphite grows concentrically in the bubble to be a graphite nodule. Then, the graphite nodule is surrounded by an austenite shell. It depends on the presence of the thin liquid channel whether the graphite nodule grows into C/V or spheroidal graphite. That is to say, the graphite nodule becomes C/V graphite if the channel is connected to the graphite, while it becomes spheroidal graphite if not.

Contribution of Thin Liquid Channel to C/V Graphite Growth

Regarding the spheroidal graphite growth in austenite shell, investigators[2,6,52] mainly explained it by the carbon atom diffusion into graphite phase. The iron atom diffusion should be, however, taken into account because of two reasons:

1) The site, where carbon precipitates as graphite around the nodule, must be formed by the iron atom diffusion. Unless the iron atoms adjacent to the graphite nodule are transported, it would not be able to grow further.
2) The diffusion transport of the iron atom is slower than that of the carbon atom at the eutectic temperature range.

At any rate, it may be true that the growth of spheroidal graphite surrounded by austenite shell is diffusion controlled by iron atom. The same mechanism can be adopted to the C/V graphite growth in austenite shell. In the case of the spheroidal graphite growth, it is considered that the iron atom is likely to evenly diffuse around graphite nodule through austenite shell and carbon atom may behave in the same way because graphite

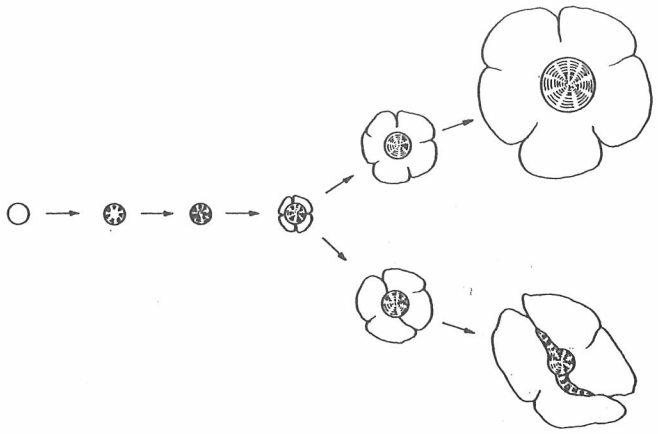

Fig. 13. Schematical illustration of the C/V and spheroidal graphite formation process.

nodule is completely isolated from the melt. Thus, graphite nodule is possible to grow into spheroidal graphite. On the other hand, in the case of C/V graphite growth, it is considered as follows. The effective diffusion coefficient (Deff) during C/V graphite growth is given by equation (1), since C/V graphite is connected to the melt through the thin liquid channel in austenite shell.

$$Deff = \alpha \cdot D_{Liq} + (1-\alpha) \cdot D_L \quad (1)$$

where D_{Liq}: Diffusion coefficient in liquid
D_L: Diffusion coefficient for the lattice diffusion.

Diffusion of iron atom in liquid and austenite lattice at 1120C (2048F) was estimated using the following values:

$D_{Liq} \cong 1 \times 10^{-6}$ cm^2/sec,[55] $D_L \cong 1 \times 10^{-11}$ cm^2/sec[55] and $\alpha = 0.001$

The probability of diffusion of iron atom through the channel is 99% and that through austenite grain is 1%. The same estimation for carbon atom diffusion at 1120C was done with these values:

$D_{Liq} \cong 4 \times 10^{-5}$ cm^2/sec,[55] $D \cong 7 \times 10^{-7}$ cm^2/sec[55] and $\alpha = 0.001$.

The probability of diffusion of iron atom through the channel is 5% and that through austenite grain is 95%. Judging from these estimations, it is obvious that growth of graphite nodule is controlled by the diffusion of iron atom, as mentioned above, and it grows preferentially through the thin liquid channel, as long as it exists in austenite shell. After all, it is essential that graphite nodule is connected to the melt through the thin liquid channel during C/V graphite growth. Although flake is said to be connected to the melt during the growth, it is directly in contact with the melt.[56] Such a difference seems to be related to that of crystallined structure between the two.

SUMMARY

The results obtained in the present work are summarized:

1) Only tiny graphite nodules precipitated at the early stage of solidification of C/V graphite cast iron, as in the case of spheroidal graphite cast iron.
2) C/V graphite was formed with the proceeding of eutectic solidification.
3) C/V graphite was connected to the melt through the thin liquid channel in austenite shell, while spheroidal graphite was completely isolated from the melt.
4) C/V graphite phases were interconnected with each other throughout austenite shell and the branches of C/V graphite were connected to original graphite nodule.
5) Impurities, such as Sn, promoted the formation of C/V graphite.
6) The growth of graphite nodule, surrounded by austenite shell, is controlled by the diffusion of iron atom and, thus, thin liquid channel within austenite shell plays an important role in the outward growth of graphite nodule.

In conclusion, the process of C/V graphite formation is explained:

1) Only tiny graphite nodule precipitates in the melt and is soon surrounded by austenite shell at the early stage of the solidification. Graphite nodule is looked upon as the primary form of C/V graphite.
2) Graphite nodule grows into C/V graphite in austenite shell with the proceeding of the eutectic solidification whenever thin liquid channel is formed in austenite shell due to the segregation of impurities during its outward growth.

REFERENCES

1. R. J. Warrick, *AFS Transactions,* vol 74, p 722 (1966).
2. K. M. Htun and R. W. Heine, *AFS Cast Metals Research Journal,* vol 5, p 51 (Jun 1969).
3. J. Siessener, W. Thury, R. Hummer and E. Nechtelbelger, *AFS Cast Metals Research Journal,* vol 8, p 178 (Dec 1972).
4. L. Sofroni, I. Ripson and I. Chira, *The Metallurgy of Cast Iron,* p 97 (1974).
5. N. N. Aleksandrov, B. S. Mil'man, N. G. Osaka, L. V. Il'icheva and V. V. Andreev, *Russian Casting Production,* p 365 (Sep 1975).
6. N. N. Aleksandrov, B. S. Mil'man, L. V. Il'icheva and N. G. Osada, *Litenoe Proizvadstvo, 8,* p 12 (1976).
7. E. R. Evance, J. V. Dawson and M. J. Lalich, *AFS International Cast Metals Journal,* vol 1, p 13 (Jun 1976).
8. K. H. Riemer, *Giesserei,* vol 63, no. 10, p 281 (1976).
9. M. M. Levitan, A. D. Kulikova, V. D. Kosynkin, V. V. Suprunko and S. D. Moiseev, *Russian Casting Production,* p 190 (May 1976).
10. F. K. Bobylev, A. S. Glinkin, N. N. Aleksandrov and V. I. Popov, *Russian Casting Production,* p 445 (Nov 1976).
11. G. F. Ruff and J. F. Wallace, *AFS Transactions,* vol 85, p 167 (1977).
12. K. P. Cooper and C. R. Loper, Jr., *AFS Transactions,* vol 86, p 267 (1978).

vol 3, p 23 (1978).
14. R. R. Oathout, *Metal Progress,* p 54 (May 1978).
15. G. F. Ruff and T. C. Vert, *AFS Transactions,* vol 87, p 459 (1979).
16. P. A. Green and A. J. Tomas, *AFS Transactions,* vol 87, p 567 (1979).
17. G. F. Sergeant, *BCIRA Journal,* vol 28, p 153 (May 1980).
18. P. C. Liu, C. R. Loper, Jr., T. Kimura and H. K. Park, *AFS Transactions,* vol 88, p 97 (1980).
20. C. R. Loper, Jr., J. J. Lalich, H. K. Park and A. M. Gyarmaty, *AFS Transactions,* vol 88, p 313 (1980).
21. T. Kimura, C. R. Loper, Jr. and H. H. Corell, *AFS Transactions,* vol 88, p 443 (1980).
22.- 30. Oriental publications
31. A. Ikenaga, T. Ueda and K. Okabayashi, *Imono,* vol 53, p 3, (Oct 1981).
32. K. Ogi, E. N. Pan and C. R. Loper, Jr., The 101st Grand Lecture Meeting of the Japan Foundrymen's Society, p 78 (1982).
33. K. Ikawa and T. Ohide, The 101st Grand Lecture Meeting of the Japan Foundrymen's Society, p 19 (1982).
34. O. Yanagisawa and T. S. Lui, *Imono,* vol 54, p 27 (May 1982).
35. T. Ohide, G. Ohira and K. Ikawa, *Imono,* vol 54, p 27 (May 1982).
36. Y. Tsunekawa and T. Shinozawa, *Imono,* vol 54, p 3 (Jul 1982).
37. N. Tsutsumi and M. Imamura, *Metals and Technology, Extra,* p 86 (Feb 1982).
38. Y. Harada, T. Tawarada, A. Nakayasu and H. Itofuji, The 67th Ductile Cast Iron Conference (in Japan), (Oct 1982).
39. E. Nechtelberger, H. Phur, J. B. von Nesselrode and A. Nakayasu, 49th International Foundry Congress, Chicago (Apr 1982).
Gusseisen mit Lamellengraphit/Kugelgraphit/Vermicular graphit im Temperaturbereich bis 500C (1982).
41. S. Yamamoto, B. Chang, Y. Kawano, R. Ozaki and Y. Murakami, *Metal Science,* 9, p 360 (1975).
42. S. Yamamoto, Y. Kawano, Y. Murakami, B. Chang and R. Ozaki, *AFS Transactions,* vol 83, p 217 (1975).
43. B. Chang, S. Yamamoto, Y. Kwano and R. Ozaki, *Imono,* vol 49, p 269 (May 1977).
44. B. Chang, S. Yamamoto, Y. Kawano and R. Ozaki, *Journal of the Japan Institute of Metals,* vol 41, 5, p 464 (1977).
45. B. Chang, S. Yamamoto, Y. Kawano and R. Ozaki, *Journal of the Japan Institute of Metals,* vol 41, 5 p 471 (1977).
46. B. Chang, S. Yamamoto, Y. Kawano and R. Ozaki, *Journal of the Japan Institute of Metals,* vol 41, 5, p 479 (1977).
47. B. Chang, S. Yamamoto, Y. Kawano and R. Ozaki, *Journal of the Japan Institute of Metals,* vol 41, 6, p 564 (1977).
48. B. Chang, S. Yamamoto, Y. Kawano and R. Ozaki, *Journal of the Japan Institute of Metals,* vol 41, 6, p 571 (1977).
49. B. Chang, S. Yamamoto, Y. Kawano and R. Ozaki, *Journal of the Japan Institute of Metals,* vol 41, 10, p 1019 (1977).
50. B. Chang, S. Yamamoto, Y. Kawano and R. Ozaki, *Journal of the Japan Institute of Metals,* vol 41, 10, p 1025 (1977).
51. S. Wetterfall, H. Fredriksson and M. Hillert, *Journal of Steel Institute,* 210, p 323 (1972).
52. J. D. Schobel, Recent Research on Cast Iron, p 303 (1968).
53. H. Horie, *Imono,* vol 49, p 3 (Jul 1976).
54. B. Chalmars, *Principles of Solidification,* p 154 (1964).
55. The Japan Institute of Metals, *Metals Hand Book,* (1974).
56. H. Morrouh, *British Foundrymen,* L 111, 5, p 321 (1960).